IEEE Photonics Journal
An IEEE Photonics Society Publication

Open Access

Nanoscale Optical Logic Circuits by Single-Step FRET

Volume 12, Number 2, April 2020

Jinya Inoue
Takahiro Nishimura
Yusuke Ogura
Jun Tanida

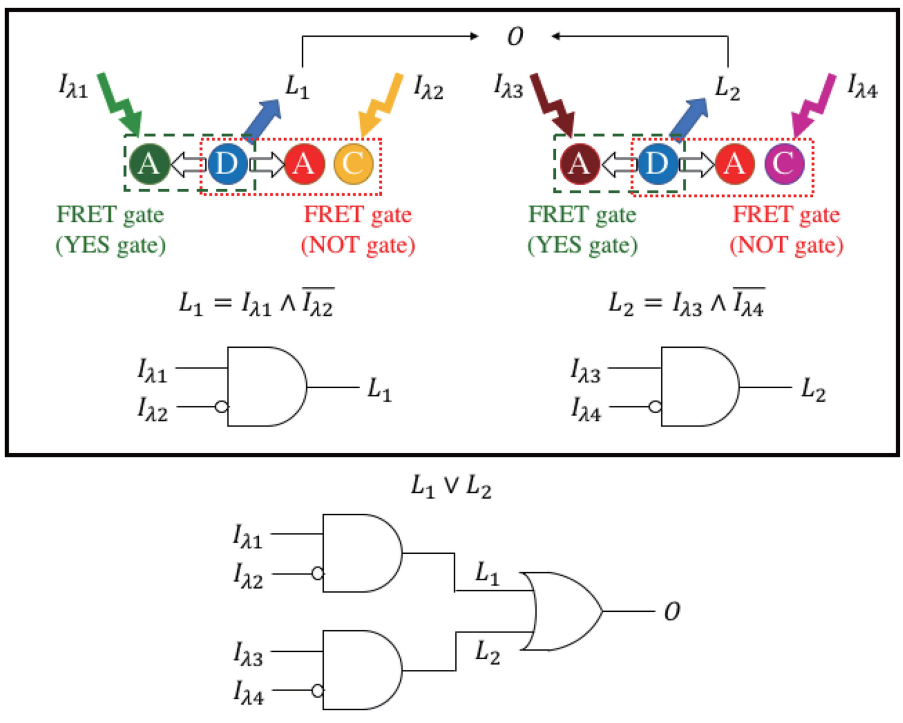

Examples of implementing AND and OR circuits with single-step FRET

DOI: 10.1109/JPHOT.2020.2976489

Nanoscale Optical Logic Circuits by Single-Step FRET

Jinya Inoue,[1] **Takahiro Nishimura**,[2] **Yusuke Ogura**,[1] **and Jun Tanida**[1]

[1]Department of Information and Physical Sciences, Graduate School of Information Science and Technology, Osaka University, Suita, Osaka 565-0871, Japan
[2]Division of Sustainable Energy and Environmental Engineering, Graduate School of Engineering, Osaka University, Suita, Osaka 565-0871, Japan

DOI:10.1109/JPHOT.2020.2976489

Manuscript received January 6, 2020; revised February 19, 2020; accepted February 23, 2020. Date of publication February 27, 2020; date of current version February 12, 2020. This work was supported by JSPS KAKENHI Grant Number JP17H02084. Corresponding author: Jinya Inoue (e-mail: j-inoue@ist.osaka-u.ac.jp).

Abstract: We propose a method for implementing nanoscale optical logic circuits via single-step Förster resonance energy transfer (FRET). Use of single-step FRET enabled circuits with simple design and high expandability. Two kinds of FRET gates, a YES gate and a NOT gate, were used to modulate fluorescence output signals based on light inputs. Various logic circuits could be implemented by connecting FRET gates on a DNA structure. The experimental results demonstrated that FRET gates for two kinds of input lights were constructed, and that logic circuits executing the AND and OR operations produced fluorescence signals as outputs.

Index Terms: Förster resonance energy transfer, optical circuit, fluorescence, DNA self-assembly.

1. Introduction

Förster resonance energy transfer (FRET) is a phenomenon describing energy transfer between fluorophores in proximity. The transfer efficiency depends on the sixth power of the distance between the fluorophores, and typically, FRET only occurs for the distance < 10 nm [1]. This attribute is attractive as a tool in bioscience [2], and is particularly useful for sensing specific molecules [3]–[8] and molecular-scale phenomena [9], [10].

Various compounds can be arranged with an interval in the order of 1 nm via self-assembly of DNA strands [11]–[13] with appropriately designed sequences. The method allows for control of the FRET mode by placing fluorophores at the desired positions. This approach offers a method for information transfer at the nanoscale. For example, nanowires that transfer energy through fluorophores on a DNA nanostructure have been developed [14]–[16]. FRET is also promising for information technology applications. To date, nano-sized routers [17], [18], memories [19], [20], and rulers for measuring the distance between substances [21]–[23] have been reported.

The combination of DNA nanotechnology with FRET is expected to be a promising way to realize molecular-scale computing. Optical circuits implemented based on this concept with fluorophores [24]–[29] and quantum dots [30], [31] have been shown to work in wet environments, and thus, they will provide new methods for cell measurement and control. In this kind of circuits, information of light and/or DNA is processed. A good example for these circuits includes nanoscale

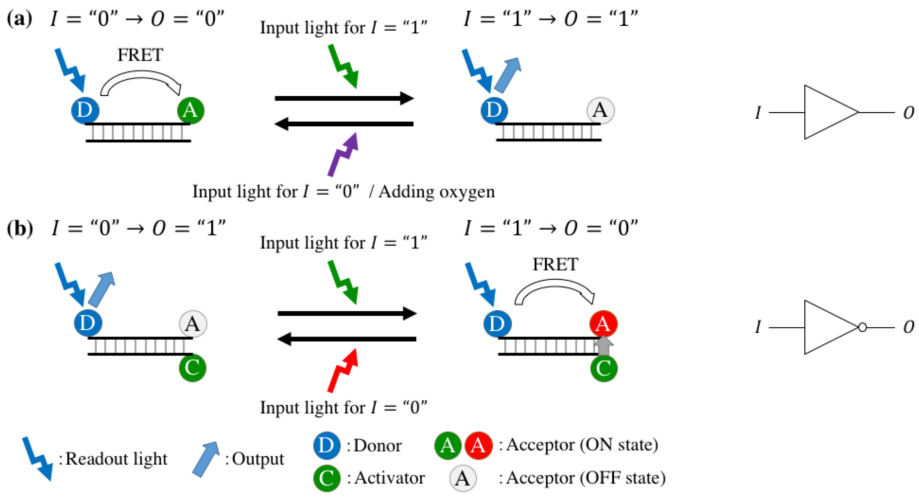

Fig. 1. Scheme of (a) a YES gate and (b) a NOT gate. Light irradiation was used for the input and the output was the donor fluorescence. Both the input and output could be represented by a binary value. The output fluorescence was modulated by switching the acceptor state using input light or by adding oxygen. The ON-state acceptors are colored by the wavelength of light that acts on each acceptor.

optical logic circuits. These circuits output a fluorescent signal for an input signal expressed by light parameters or the presence of DNA [26], [28]. The FRET paths constructed in these circuits are modified according to the inputs, and the output signals are generated as the result of a previously set logic operation. By designing circuits where multiple FRET steps occur, two-input one-output logic operations can be executed [29]. Logic circuits that deal with three or more inputs have also been demonstrated [25]. However, the structures of multi-step-FRET circuits tend to be complicated. This restricts the expandability of the circuits and the realization of more advanced computing operations.

In this paper, we propose optical circuits based on single-step FRET assembly. Using this strategy, the structure of the circuit can be simplified and therefore it affords high expandability. In addition, energy dissipation because of consecutive FRET steps is avoidable. Two kinds of FRET gates were used for implementing the circuits based on single-step FRET. Combining these gates enables the implementation of a logical formula in the disjunctive normal form, and therefore various logic operations can be executed. The properties of the fabricated FRET gates were investigated and logic operations were then demonstrated to confirm the validity of the proposed method.

2. Scheme

The input of the proposed circuits is a set of binary light signals and the output is also a binary fluorescent signal. The output is $O =$ "0" when the output intensity is low and $O =$ "1" when it is high. The intensity is modulated by changing the FRET paths that are constructed, which depends on the state of the fluorophores controlled by input light I. The input I is controlled by two lights forming $I =$ "1" and $I =$ "0".

A YES gate and a NOT gate were used as primary components to implement various logic circuits. The scheme of the gates is shown in Fig. 1. The YES gate and the NOT gate detect one input and produce one output. The output fluorescence intensity is modulated in response to the input light. These two gates are referred to as FRET gates in this paper. Previous methods proposed using fluorescence from an acceptor as the output [24]–[29]. If the result of a circuit is obtained from an acceptor, the number of FRET steps must be the same as the number of inputs for constructing an AND circuit. In contrast, this work used the fluorescence from a donor as the output signal of the FRET gates, which enabled the construction of circuits using single-step FRET.

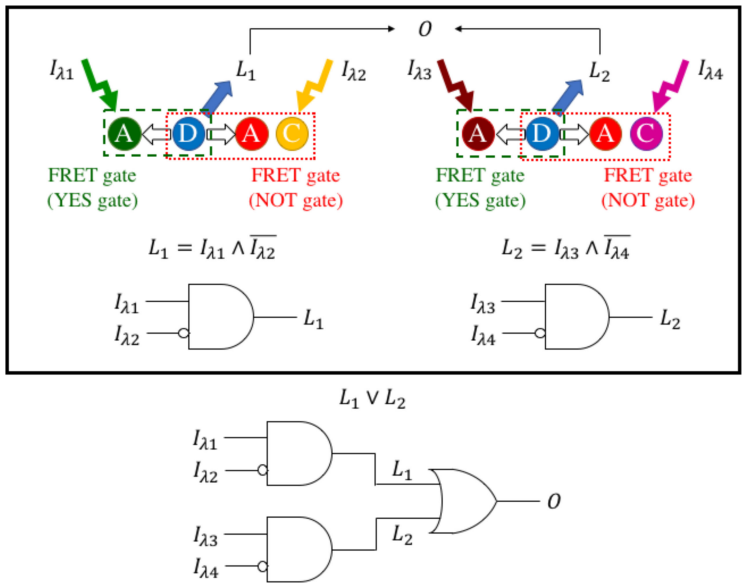

Fig. 2. Examples of implementing AND and OR circuits. *D* donor, *A* acceptor, *C* activator, *O* output. Hollow arrows represent FRET. The left part is a logic circuit that executes an AND operation L_1, and the right part executes an AND operation L_2. Using these two circuits simultaneously, an OR circuit that executes $L_1 \vee L_2$ could be implemented (inside of the black frame).

The YES gate was composed of a FRET pair of two fluorophores, a donor (D) and an acceptor (A) which is an optically switchable fluorophore. As shown in Fig. 1(a), the FRET path of the YES gate is a single step. The input light for $I =$ "1" of the YES gate acts on the acceptor, switching it from the ON state to the OFF state. Then, the FRET efficiency from the donor to the acceptor decreases, and the output intensity from the donor increases. The output fluorescence intensity produced from the YES gate increases when *I* is switched from "0" to "1". The acceptor is returned to the ON state by irradiation for $I =$ "0" or by adding oxygen. Then, the YES gate state returns to "0".

In contrast, the output fluorescence intensity from the NOT gate decreases when *I* is switched from "0" into "1". The NOT gate is composed of three fluorophores, a donor, an acceptor and an activator (C), as shown in Fig. 1(b). The NOT gate also had a single-step FRET path. The activator was placed near the acceptor. The acceptor was in the OFF state when $I =$ "0". The input light of $I =$ "1" of the NOT gate operates on the activator. If the activator is optically excited, it turns the acceptor from the OFF state to the ON state [32]. As a result, a FRET path from the donor to the acceptor is formed, and the donor output intensity decreases. The acceptor state returns to the OFF state on irradiation. This causes the state of the NOT gate to subsequently return to "0". The ON and OFF states depend on the quantum state of the acceptor, the singlet or the triplet state, and the existence of the thior group in the fluorophore polymethine structure [33], [34]. Oxygen and the activator change the quantum state and the existence of the thior group. The activator is necessary for switching the OFF-state acceptor to the ON state by the same light for $I =$ "1" as the YES gate. The activator of the NOT gate can also work as an acceptor. However, only single-step FRET is necessary for obtaining the output even if there are two acceptors in a NOT gate.

The fluorophores of the FRET gates were placed on a DNA structure. Nanoscale optical logic circuits were constructed by connecting the FRET gates via DNA self-assembly. Fig. 2 shows examples of the AND and OR circuits. An AND circuit could be implemented by connecting the FRET gates by sharing a single donor. An OR circuit could be implemented by simultaneously using different kinds of FRET gates and/or AND circuits. The output of $L_1 \vee L_2$ is the sum of fluorescence intensities from the donors of L_1 and L_2. Various logic operations in the disjunctive normal form can be implemented by proper simultaneous utilization of YES gates and/or NOT gates. The number of input variables can be increased by using FRET gates with different input light wavelengths.

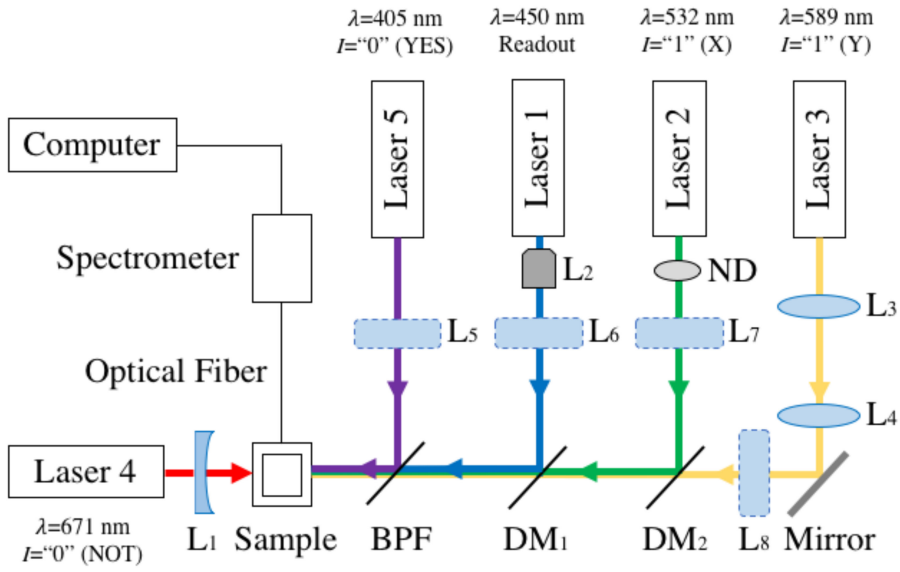

Fig. 3. The optical system of experiments. This figure describes two optical setups, for a 30-μL sample and for a 10-μL sample. L_1 is a concave lens (the focal length is 80 mm). L_2 is an objective lens (the magnification is 10). L_3 and L_4 are convex lenses (with focal lengths of 40 mm and 160 mm), which form a beam expander. L_5 is a convex lens with a focal length of 120 mm (when the sample volume is 30 μL) or 150 mm (10 μL). L_6 is blank (30 μL) or a convex lens (for 10 μL, the focal length is 260 mm). L_7 is an objective lens (for 30 μL, the magnification is 4) or a convex lens (for 10 μL, the focal length is 450 mm). L_8 is blank (30 μL) or a convex lens (for 10 μL, the focal length is 350 mm). *BPF* band pass filter, *DM* dichroic mirror, *ND* neutral density filter.

The number of output variables can also be increased by using circuits that have different donor fluorophores. Furthermore logic gates can be connected sequentially when the emission peak wavelength of the donor of the former gate and the absorption peak wavelength of the acceptor (YES gate) or the activator (NOT gate) of the latter gate are similar. The limitation that the count of connection steps is limited due to the difference between input and output wavelength is common in FRET-based circuits. However, because our method uses a fluorescence signal from the donor as output, the limitation is alleviated comparing to logic circuits using multi-step FRET, which uses an acceptor as output.

3. Optical Setup

The optical setup is shown in Fig. 3. The used optical system depended on the volume of the sample. Fig. 3 combines two cases. The lenses used were chosen according to the volume of the sample to adjust the laser diameter to the surface area of the samples.

Five laser sources were used to modulate and measure the state of the gates or circuits. The sample was placed in a glass stick cell. Then the fluorescence spectra from the sample were measured using a spectrometer (BTC112E, B& W Tek, Inc.,). The beams from the laser sources were combined to share the optical axis using a mirror, dichroic mirrors, and a band pass filter. Following this, the sample was irradiated with the laser sources. The fluorescence emission from the sample was collected by the detector (attached with the spectrometer) set close to the sample, and sent to the spectrometer through the optical fiber. Laser 1($\lambda = 450$ nm, L450P1600MW, Thorlabs) was used to readout the output fluorescence of the FRET gates and the optical logic circuits. The light from Laser 2 ($\lambda = 532$ nm, Excelsior-CDRH, Spectra-Physics) and Laser 3 ($\lambda = 589$ nm, OEM-U-589-100mW-18041236, Changchun New Industries Optoelectronics Tech.Co., Ltd.) were used as an input for $I =$ "1" to the FRET gates and circuits. Laser 4 ($\lambda = 671$ nm, SDL-671-400 T, Shanghai Dream Lasers Technology Co., Ltd.) was the input light for $I =$ "0" of the NOT gates. Laser

5 ($\lambda = 405$ nm, Violet Laser Module, Laserlands) was the input light for $I =$ "0" of the YES gate [35], [36]. Additionally, the acceptor returned to the ON state if the sample was left unperturbed for 3 minutes. This is referred to as natural recovery in this work and was used for the YES gate.

4. Experiments on FRET Gates

4.1 Experimental Condition

For implementing an optical logic circuit with two inputs and one output, FRET gates were prepared that functioned with input lights of different wavelengths.

The FRET gate sample consisted of some DNA strands and reagents. The DNA strands were purchased from Japan Bio Services CO., LTD and Tsukuba Oligo Service CO., LTD. The sample of a YES gate consisted of 3.3×10^{-6}-M donor-attached DNA (10 mer), 3.3×10^{-6}-M acceptor-attached DNA (10 mer), 3.3×10^{-6}-M scaffold DNA (20 mer) for fixing the distance between the donor and the acceptor, 0.1-M mercaptoethylamine (MEA), and 8.3×10^{-2}-M NaOH. The sample of a NOT gate consisted of 3.3×10^{-6}-M DNA with a donor and an acceptor attached to both ends (10 mer), 6.6×10^{-6}-M activator-attached DNA (10 mer), 0.1-M MEA, and 8.3×10^{-2}-M NaOH. With this concentration, the effect of collisional FRET is considered to be negligible [37]. The pair of NaOH and MEA is necessary for photoswiching of fluorophores [24]. The DNA and reagents were mixed in the buffer. The buffer contains 0.005-M Tris-HCl, 1-M NaCl, 0.01-M $MgCl_2$, 100-mg/mL glucose, 0.04-mg/mL catalase, and 0.5-mg/mL glucose oxidase. Catalase and glucose oxidase are used for photoswitching of fluorophores.

Four kinds of FRET gates were fabricated. Alexa Fluor 488 (AF488; Abs: 495 nm, Em: 520 nm) was selected as the donor for all the FRET gates. The FRET gates were classified not only by a YES gate and a NOT gate, but also by the input light for $I =$ "1". Lights of two wavelengths at 532 nm and 589 nm were used as the input lights for $I =$ "1". FRET gates with an input wavelength for $I =$ "1" of 532 nm were classified into group X. If the wavelength was 589 nm, the FRET gate was classified in the group Y. The YES gate and the NOT gate were implemented for both groups. The YES gate and the NOT gate of group X are referred to as $YES^{(X)}$ gate and $NOT^{(X)}$ gate, respectively. Similarly, the YES gate and the NOT gate of group Y are referred to as the $YES^{(Y)}$ gate and the $NOT^{(Y)}$ gate, respectively. The structures of the FRET gates and the base sequences of the DNA strands used are shown in Fig. 4. The acceptors of the YES gates and the activators of the NOT gates were selected for their response to the specific wavelengths of the input lights for $I =$ "1". Alexa Fluor 532 (AF532; Abs: 532 nm, Em: 553 nm) and Cy3.5 (Abs: 581 nm, Em: 596 nm) were the acceptors for the $YES^{(X)}$ gate and the $YES^{(Y)}$ gate, respectively. Cy3 (Abs: 550 nm, Em: 570 nm) and Alexa Fluor 568 (AF568; Abs: 578 nm, Em: 603 nm) were the activators for the $NOT^{(X)}$ gate and the $NOT^{(Y)}$ gate, respectively. Cy5 (Abs: 643 nm, Em: 667 nm), whose state is optically controllable [34], was used as the acceptor of the NOT gates. An acceptor and an activator were arranged at the same side of the DNA strands to obtain the effect of the activator [33]. For all gates, the distance between the donor and acceptor was designed to be 10 mers. In both the YES and the NOT gates, the different parts between the group X and Y (YES gate; the acceptor, NOT gate; the activator) were separated to compose the FRET gates and the circuits with common DNAs as possible. The intensity and irradiation time of the used lights are shown in Table 1. The 450-nm light was used to read the output for all gates. The other wavelengths were selected in accordance with the individual fluorescence molecules. The $YES^{(X)}$ gate was set to the "0" state using oxygen. A 10-μL sample was prepared in the experiment using the $YES^{(Y)}$ gate, and a sample volume of 30 μL was used for the other experiments.

4.2 Experimental Results

First, four kinds of FRET gates were investigated, which were used as components for nanoscale optical logic circuits. The change in the output fluorescence intensity when $I =$ "0" and $I =$ "1" was measured.

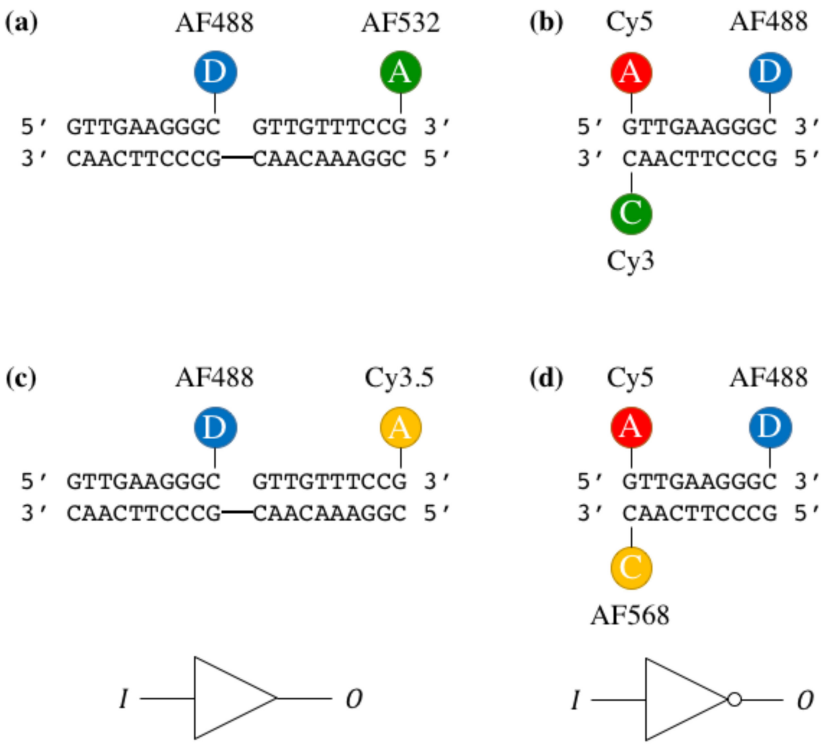

Fig. 4. The structures of FRET gates, (a) YES$^{(X)}$, (b) NOT$^{(X)}$, (c) YES$^{(Y)}$, (d) NOT$^{(Y)}$ gate. *D* donor, *A* acceptor, and *C* activator.

TABLE 1
The Power Density and Irradiation Time of the Lights Used in FRET Gates. The YES$^{(X)}$ Gate was Set to I = "0" by Adding Oxygen

The type of the gate	Role	Wavelength [nm]	Power Density [W/cm^2]	Irradiation time
YES$^{(X)}$, NOT$^{(X)}$, NOT$^{(Y)}$	Readout	450	2.55×10^{-3}	10 sec.
YES$^{(Y)}$	Readout	450	15.9×10^{-3}	10 sec.
YES$^{(X)}$	I="1"	532	0.112	30 sec.
YES$^{(Y)}$	I="1"	589	1.273	5 min.
YES$^{(Y)}$	I="0"	405	0.796	30 sec.
NOT$^{(X)}$	I="1"	532	0.336	30 sec.
NOT$^{(X)}$	I="0"	671	0.815	4 min.
NOT$^{(Y)}$	I="1"	589	0.285	30 sec.
NOT$^{(Y)}$	I="0"	671	0.815	6 min.

The measured raw spectrum was considered to be the weighted sum of two or three fluorophore spectra. The spectrum was separated into the primary spectra based on the following fitting procedure. The spectra of the individual fluorophores were measured first. If three types of fluorophores (a donor, an acceptor, and an activator) are present in the sample, the obtained spectrum can be expressed via the following expression.

$$S_{fit}(\lambda) = k_D \cdot S_D(\lambda) + k_A \cdot S_A(\lambda) + k_C \cdot S_C(\lambda), \tag{1}$$

where $S_{fit}(\lambda)$ is the spectrum after separation. $S_D(\lambda)$, $S_A(\lambda)$, and $S_C(\lambda)$ are the fluorescent spectra of the donor, the acceptor, and the activator, respectively, after subtracting the buffer spectrum. $S_D(\lambda)$, $S_A(\lambda)$, and $S_C(\lambda)$ were measured individually in advance. The buffer spectrum is the spectrum from the glucose oxidase under the blue light (readout light) irradiation. k_D, k_A, k_C are the coefficient

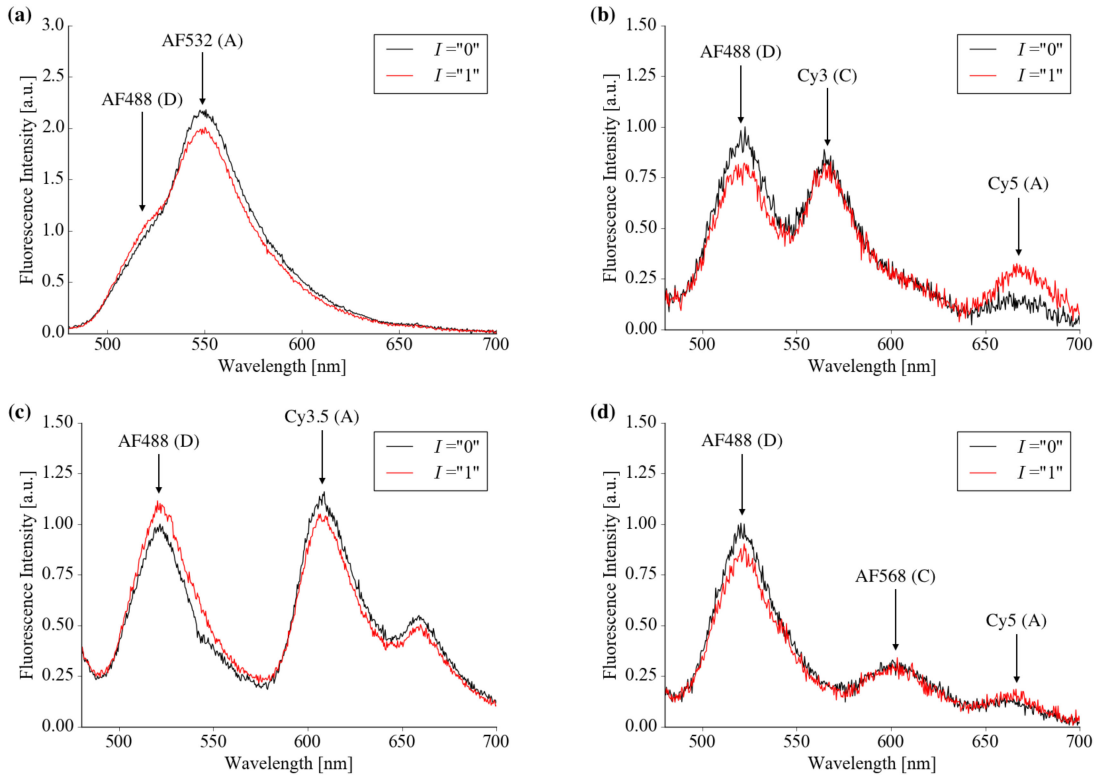

Fig. 5. The raw spectra of FRET gates [(a): YES$^{(X)}$, (b): NOT$^{(X)}$, (c): YES$^{(Y)}$, (d): NOT$^{(Y)}$ gate] when I = "0" and I = "1". (D), (A), (C) in the figures stand for the donor, the acceptor, and the activator.

for the donor, the acceptor, and the activator, respectively. When the spectrum of a YES gate is measured, the $S_C(\lambda)$ term is eliminated from Eq. (1). The buffer spectrum was subtracted from the raw spectrum of the FRET gate. The spectrum obtained after subtraction is $S_{obt}(\lambda)$. The coefficients that minimize

$$\int \left\{ S_{obt}(\lambda) - S_{fit}(\lambda) \right\}^2 d\lambda \tag{2}$$

were calculated. Then, the output intensity of the FRET gate was estimated by multiplying the coefficient with the value at the fluorescence peak wavelength of the donor fluorescent spectrum.

The raw spectra when I = "0" (black curve) and I = "1" (red curve) of the four FRET gates are shown in Fig. 5. These spectra were normalized using the peak value of the donor fluorescence when I = "0". The relative intensities averaged over two measurements and its standard deviations were measured. The output intensity of the YES$^{(X)}$ gate for I = "1" increased by 30.8 $\pm$ 1.3% compared with I = "0". For the NOT$^{(X)}$ gate, the output decreased by 17.6 $\pm$ 2.3%. For the YES$^{(Y)}$ and the NOT$^{(Y)}$ gates, the output increased by 13.9 $\pm$ 1.3% and decreased by 14.0 $\pm$ 0.9%, respectively. These results demonstrate that the designed FRET gates produced fluorescent outputs that depended on the input lights. As seen from Fig. 5, the donor and acceptor fluorescence intensities move in opposite directions. These results indicate that the FRET paths were altered depending on the input lights. The differences of the signal-to-noise-ratio (SNR) among the gates are due to the differences among the intensities of the spectra of raw data before normalization.

Next, the output fluorescence intensity of the FRET gates were investigated to see if they change with consecutive inputs. The input of the FRET gates was varied continuously by alternately irradiating the sample with the input signal or it was allowed to recover naturally. The output was measured each time the input was changed. The output fluorescence intensities were normalized

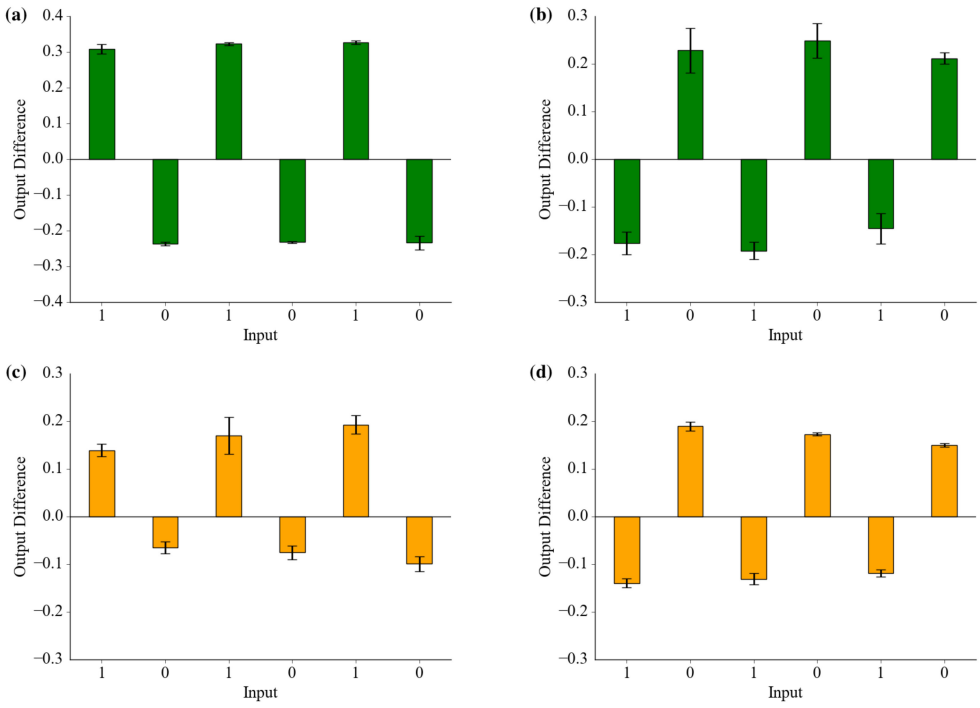

Fig. 6. Consecutive changes of output fluorescence intensity of the FRET gates [(a): YES$^{(X)}$, (b): NOT$^{(X)}$, (c): YES$^{(Y)}$, (d): NOT$^{(Y)}$ gate] according to the input state. The values are ones averaged over two measurements, and the error bars show standard deviations. The vertical axis represents the differences of the output fluorescence intensity compared with the previous state.

using the intensity of the first I = "0" state. Because of photobleaching, the OFF-state acceptors did not completely return to the ON state. To eliminate the influence of the photobleaching, the difference of the output from the previous state was evaluated. The output differences of the YES gates were expected to be a positive when I = "1," and to be negative when I = "0". In contrast, those of the NOT gates were expected to be negative when I = "1" and to be positive when I = "0". The relationship between the input and the output differences are shown in Fig. 6. For all the FRET gates, the results indicated that the output changes occurred in three cycles.

FRET gates with two kinds of input lights were demonstrated. These gates can be implemented using the same layout by selecting fluorophores for different input light wavelengths.

5. Investigation of Nanoscale Optical Logic Circuits

5.1 Experimental Condition

By combining two FRET gates, nanoscale two-input one-output optical logic circuits were fabricated. The output fluorescence intensities according to a set of inputs were measured to verify the behavior of the circuits. As examples, an AND circuit and an OR circuit were implemented because these are the basic operations required for construction of a complete system. In this paper, two operations are presented: $I_X \wedge \overline{I_Y}$ and $I_X \vee I_Y$. I_X is the input of the FRET gate of the group X. I_Y is that of the group Y. The AND circuit can be implemented by connecting the YES$^{(X)}$ gate and the NOT$^{(Y)}$ gate with a common donor, as shown in Fig. 7(a). We selected this AND circuit to implement an operation including a NOT gate as a component of the disjunctive normal form. The OR circuit can be implemented using the YES$^{(X)}$ gate and the YES$^{(Y)}$ gate simultaneously, as shown in Fig. 7(b).

The AND circuit sample consisted of 3.3×10^{-6}-M DNA with an AF488 and a Cy5 attached to both ends (10 mer), 3.3×10^{-6}-M AF532-attached DNA (10 mer), 6.6×10^{-6}-M

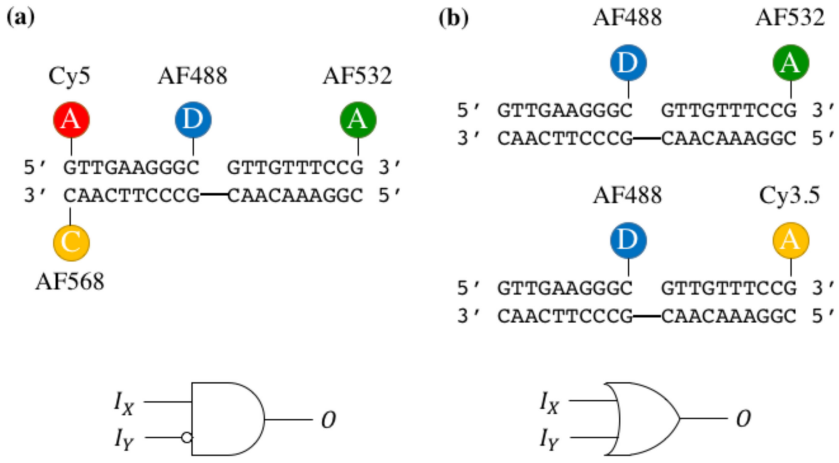

Fig. 7. (a) The structure of the AND circuit $I_X \wedge \overline{I_Y}$. The left part including the donor is the NOT$^{(Y)}$ gate, and the right part including the donor is the YES$^{(X)}$ gate. (b) The structure of the OR circuit $I_X \vee I_Y$. Sequences were designed to prevent two YES gates from binding to each other. *D* donor, *A* acceptor, and *C* activator.

TABLE 2
The Power Density and Irradiation Time of the Lights Used in the Circuits

The type of the circuit	Role	Wavelength [nm]	Power Density [W/cm^2]	Irradiation time
AND	Readout	450	2.55×10^{-3}	10 sec.
OR	Readout	450	15.9×10^{-3}	10 sec.
AND	I_X="1"	532	0.153	30 sec.
AND	I_Y="1"	589	0.143	30 sec.
AND	I_Y="0"	671	0.688	6 min.
OR	I_X="1"	532	0.446	30 sec.
OR	I_Y="1"	589	1.273	5 min.

AF568-attached DNA (20 mer), 0.1-M MEA, and 8.3×10^{-2}-M NaOH. The OR circuit sample consisted of 6.6×10^{-6}-M AF488-attached DNA (10 mer), 3.3×10^{-6}-M AF532-attached DNA (10 mer), 3.3×10^{-6}-M Cy3.5-attached DNA (10 mer), 6.6×10^{-6}-M scaffold DNA (20 mer), 0.1-M MEA, and 8.3×10^{-2}-M NaOH. The DNA and reagents were mixed in the buffer. The buffer was the same as the experiments for the FRET gates. The volume of the AND circuit and the OR circuit were 30 μL and 10 μL, respectively. Sequences of the DNA used are shown in Fig. 7. The intensity and the irradiation time of the used lights are shown in Table 2. The used optical system was the same as that shown in Fig. 3.

5.2 Experimental Results

First, the output fluorescence intensity for each input was investigated. The input of the sample was set to (I_X, I_Y) = (0, 0) initially, and then it was switched to the desired one. The output intensities measured for each input state are shown in Fig. 8. The intensities were averaged over three measurements and normalized using the output intensity for the (0, 0) input state. From Fig. 8, for both circuits, the responses were reasonably in agreement with the designed operation. By using a suitable threshold value, for example the average value of the maximum output intensity for O = "0" and the minimum intensity for O = "1," correct binary values of the output for a single circuit could be obtained when considering the average of the output. To determine an absolute threshold value for a more complicated circuit, it is necessary to improve the performance of the gates. The output intensity of the AND circuit had a maximum value with an input of (1, 0) and a minimum for an input (0, 1); this was because both the YES$^{(X)}$ and NOT$^{(Y)}$ gates had O = "1" (input (1, 0)) or O

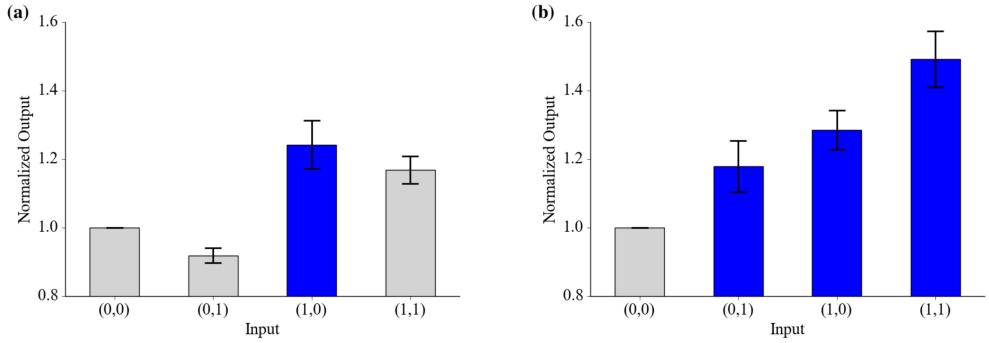

Fig. 8. Output fluorescence intensity of (a) the AND circuit $I_X \wedge \overline{I_Y}$ and (b) the OR circuit $I_X \vee I_Y$ according to the input light patterns. The values are ones averaged over three measurements, and the error bars show standard deviations. The horizontal axes are the input light pattern (I_X, I_Y). The blue and the gray graphs represent the $O =$ "1" and $O =$ "0" states, respectively.

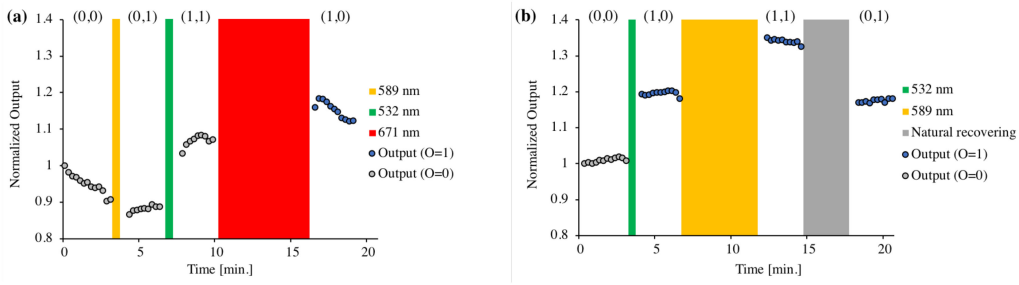

Fig. 9. Consecutive changes of the output fluorescence intensity of (a) AND circuit $I_X \wedge \overline{I_Y}$ and (b) OR circuit $I_X \vee I_Y$. The numbers in the top of figures are the input states (I_X, I_Y). The yellow, green, and red parts represent the irradiating state with the input light. The gray part is the natural recovery state.

$=$ "0" (input (0, 1)). The output for input (1, 1) showed relatively high intensity because the effect of I_X is greater than I_Y. As mentioned in Subsection 4.2, the ratio of output change of the YES$^{(X)}$ was 30.8% and that of the NOT$^{(Y)}$ gate was 14.0%. Thus, the difference of the output fluorescence intensities between (1, 0) and (0, 0) or (0, 1) is larger than the difference between (1, 0) and (1, 1). In the OR circuit, the output intensity had a maximum for an input (1, 1) because both YES$^{(X)}$ and YES$^{(Y)}$ gates were in the $O =$ "1" state. The output had a minimum for the input (0, 0) because both the YES gates were in the $O =$ "0" state.

The consecutive changes of the output fluorescence intensities of the AND and the OR circuits in response to multiple sequential inputs were measured to evaluate a time response of the circuits. The readout light was continuously irradiated on the sample. The input state was changed every three minutes by irradiation with the input light or by natural recovery. The output intensities were measured every 15 s with an exposure time of 10 s. Additionally, measurement of the AND circuit was started 1 min after the beginning of the readout light irradiation to reduce the attenuation of the output fluorescence intensity. The input state of the AND circuit was changed to (0, 0), (0, 1), (1, 1), and (1, 0) in turn. That of the OR circuit was changed to (0, 0), (1, 0), (1, 1), and (0, 1) in turn. The measurement results are shown in Fig. 9. The output intensities were normalized using that for the initial (0, 0) state. In the AND circuit, the output intensity had a maximum when the input was (1, 0) and a minimum for the (0, 1) state. In the OR circuit, the output intensity had a maximum when input was (1, 1) and a minimum for the (0, 0) state, similar to the previous result (Fig. 8). In both circuits, consecutive changes of the output fluorescence intensities with the input sequence were verified. It is expected that increasing light power density is a possible solution to shorten the response time of the circuits.

6. Conclusion

In this work, nanoscale optical logic circuits were proposed with single-step FRET. The components of the circuits were two kinds of FRET gates, a YES gate, and a NOT gate. By combining the FRET gates properly with DNA technology, various logic circuits could be implemented based on the disjunctive normal form. Use of the single-step FRET allows for the construction of circuits with simple structures.

The experimental results demonstrated the YES gates and the NOT gates using two different input light wavelengths for $I =$ "1" worked as expected. Moreover, the output of the FRET gates with changing input was verified. The operations of an AND circuit and an OR circuit constructed by connecting FRET gates were also demonstrated. In addition, the consecutive changes of the output could be realized with different input signal sequences.

The performance of the proposed circuit depends on the behavior of the FRET gates. For improved circuit performance and reliable operations, it is important to adjust the layout of the fluorophores in the circuits and the conditions for light irradiation, which lead increase of the FRET efficiency and switching efficiency. The countermeasure for the fluctuation of output signals depending on environment should also be made by, for example, fluorescence ratio measurements to achieve more reliable operations. The proposed method can be applied for nanoscale information systems that work in wet and nanoscale conditions, such as in cells.

References

[1] R. Roy, S. Hohng, and T. Ha, "A practical guide to single-molecule FRET," *Nature Methods*, vol. 5, no. 6, pp. 507–516, 2008.

[2] W. R. Algar, N. Hildebrandt, S. S. Vogel, and I. L. Medintz, "Fret as a biomolecular research tool—understanding its potential while avoiding pitfalls," *Nature Methods*, vol. 16, no. 9, pp. 815–829, 2019.

[3] C. Fan, K. W. Plaxco, and A. J. Heeger, "Biosensors based on binding-modulated donor-acceptor distances," *Trends Biotechnology*, vol. 23, no. 4, pp. 186–192, 2005.

[4] H. Chang, L. Tang, Y. Wang, J. Jiang, and J. Li, "Graphene fluorescence resonance energy transfer aptasensor for the thrombin detection," *Analytical Chemistry*, vol. 82, no. 6, pp. 2341–2346, 2010.

[5] S. Bi, J. Zhang, S. Hao, C. Ding, and S. Zhang, "Exponential amplification for chemiluminescence resonance energy transfer detection of MicroRNA in real samples based on a cross-catalyst strand-displacement network," *Analytical Chemistry*, vol. 83, no. 10, pp. 3696–3702, 2011.

[6] L. Yang, C. Liu, W. Ren, and Z. Li, "Graphene surface-anchored fluorescence sensor for sensitive detection of MicroRNA coupled with enzyme-free signal amplification of hybridization chain reaction," *ACS Appl. Mater. Interfaces*, vol. 4, no. 12, pp. 6450–6453, 2012.

[7] R. Venkataraj, A. Sarkar, C. P. Girijavallabhan, P. Radhakrishnan, V. P. N. Nampoori, and M. Kailasnath, "Fluorescence resonance energy-transfer-based fluoride ion sensor," *Appl. Opt.*, vol. 57, no. 15, pp. 4322–4330, 2018.

[8] A. Kaur, K. Sapkota, and S. Dhakal, "Multiplexed nucleic acid sensing with single-molecule FRET," *ACS Sensors*, vol. 4, no. 3, pp. 623–633, 2019.

[9] Y. Ma *et al.*, "A FRET sensor enables quantitative measurements of membrane charges in live cells," *Nature Biotechnology*, vol. 35, no. 4, pp. 363–370, 2017.

[10] Y. Pan *et al.*, "Genetically encoded FRET biosensor for visualizing epha4 activity in different compartments of the plasma membrane," *ACS Sensors*, vol. 4, no. 2, pp. 294–300, 2019.

[11] W. Su, V. Bonnard, and G. A. Burley, "DNA-templated photonic arrays and assemblies: Design principles and future opportunities," *Chemistry - A Eur. J.*, vol. 17, no. 29, pp. 7982–7991, 2011.

[12] Y. N. Teo and E. T. Kool, "DNA-multichromophore systems," *Chem. Rev.*, vol. 112, no. 7, pp. 4221–4245, 2012.

[13] C. Laboda, H. Duschl, and C. L. Dwyer, "DNA-enabled integrated molecular systems for computation and sensing," *Accounts Chem. Res.*, vol. 47, no. 6, pp. 1816–1824, 2014.

[14] C. M. Spillmann, S. Buckhout-White, E. Oh, E. R. Goldman, M. G. Ancona, and I. L. Medintz, "Extending FRET cascades on linear DNA photonic wires," *Chem. Commun.*, vol. 50, no. 55, pp. 7246–7249, 2014.

[15] B. Albinsson, J. K. Hannestad, and K. Börjesson, "Functionalized DNA nanostructures for light harvesting and charge separation," *Coordination Chemistry Rev.*, vol. 256, no. 21-22, pp. 2399–2413, 2012.

[16] J. K. Hannestad, S. R. Gerrard, T. Brown, and B. Albinsson, "Self-assembled DNA-based fluorescence waveguide with selectable output," *Small*, vol. 7, no. 22, pp. 3178–3185, 2011.

[17] W. Su, C. R. Bagshaw, and G. A. Burley, "Addressable and unidirectional energy transfer along a DNA three-way junction programmed by pyrrole-imidazole polyamides," *Scientific Reports*, vol. 3, 2013, Art. no. 1883.

[18] A. Toulmin *et al.*, "Conformational Heterogeneity in a Fully Complementary DNA Three-Way Junction with a GC-Rich Branchpoint," *Biochemistry*, vol. 56, no. 37, pp. 4985–4991, 2017.

[19] M. D. Mottaghi and C. Dwyer, "Thousand-fold increase in optical storage density by polychromatic address multiplexing on self-assembled DNA nanostructures," *Adv. Mater.*, vol. 25, no. 26, pp. 3593–3598, 2013.

[20] A. Saini, C. W. Christenson, T. A. Khattab, R. Wang, R. J. Twieg, and K. D. Singer, "Threshold response using modulated continuous wave illumination for multilayer 3D optical data storage," *J. Appl. Phys.*, vol. 121, no. 4, 2017, Art. no. 043101.
[21] I. H. Stein, V. Schüller, P. Böhm, P. Tinnefeld, and T. Liedl, "Single-molecule FRET ruler based on rigid DNA origami blocks," *ChemPhysChem*, vol. 12, no. 3, pp. 689–695, 2011.
[22] E. Sobakinskaya, M. Schmidtam Busch, and T. Renger, "Theory of FRET "spectroscopic ruler" for short distances: Application to polyproline," *J. Phys. Chemistry B*, vol. 122, no. 1, pp. 54–67, 2018.
[23] S. Qu, C. Liu, Q. Liu, W. Wu, B. Du, and J. Wang, "Solvent effect on FRET spectroscopic ruler," *J. Chem. Phys.*, vol. 148, no. 12, 2018, Art. no. 123331.
[24] R. Fujii, T. Nishimura, Y. Ogura, and J. Tanida, "Nanoscale energy-route selector consisting of multiple photo-switchable fluorescence-resonance-energy-transfer structures on DNA," *Opt. Rev.*, vol. 22, no. 2, pp. 316–321, 2015.
[25] T. Nishimura, Y. Ogura, and J. Tanida, "Fluorescence resonance energy transfer-based molecular logic circuit using a DNA scaffold," *Appl. Phys. Lett.*, vol. 101, no. 23, 2012, Art. no. 233703.
[26] C. D. LaBoda, A. R. Lebeck, and C. L. Dwyer, "An optically modulated self-assembled resonance energy transfer pass gate," *Nano Lett.*, vol. 17, no. 6, pp. 3775–3781, 2017.
[27] T. Nishimura, Y. Ogura, and J. Tanida, "A nanoscale set-reset flip-flop in fluorescence resonance energy transfer-based circuits," *Appl. Phys. Exp.*, vol. 6, no. 1, 2013, Art. no. 015201.
[28] T. Nishimura, R. Fujii, Y. Ogura, and J. Tanida, "Optically controllable molecular logic circuits," *Appl. Phys. Lett.*, vol. 107, no. 1, 2015, Art. no. 013701.
[29] C. LaBoda, C. Dwyer, and A. R. Lebeck, "Exploiting dark fluorophore states to implement resonance energy transfer pre-charge logic," *IEEE Micro*, vol. 37, no. 4, pp. 52–62, 2017.
[30] J. C. Claussen, W. R. Algar, N. Hildebrandt, K. Susumu, M. G. Ancona, and I. L. Medintz, "Biophotonic logic devices based on quantum dots and temporally-staggered förster energy transfer relays," *Nanoscale*, vol. 5, no. 24, pp. 12 156–12 170, 2013.
[31] J. C. Claussen, N. Hildebrandt, K. Susumu, M. G. Ancona, and I. L. Medintz, "Complex logic functions implemented with quantum dot bionanophotonic circuits," *ACS Appl. Mater. Interfaces*, vol. 6, no. 6, pp. 3771–3778, 2014.
[32] M. Bates, B. Huang, G. T. Dempsey, and X. Zhuang, "Multicolor super-resolution imaging with photo-switchable fluorescent probes," *Science*, vol. 317, no. 5845, pp. 1749–1753, 2007.
[33] M. Bates, T. R. Blosser, and X. Zhuang, "Short-range spectroscopic ruler based on a single-molecule optical switch," *Phys. Rev. Lett.*, vol. 94, no. 10, 2005, Art. no. 108101.
[34] G. T. Dempsey, M. Bates, W. E. Kowtoniuk, D. R. Liu, R. Y. Tsien, and X. Zhuang, "Photoswitching mechanism of cyanine dyes," *J. Amer. Chem. Soc.*, vol. 131, no. 51, pp. 18 192–18 193, 2009.
[35] G. T. Dempsey, J. C. Vaughan, K. H. Chen, M. Bates, and X. Zhuang, "Evaluation of fluorophores for optimal performance in localization-based super-resolution imaging," *Nature Methods*, vol. 8, no. 12, pp. 1027–1036, 2011.
[36] P. Dedecker *et al.*, "Subdiffraction imaging through the selective donut-mode depletion of thermally stable photoswitchable fluorophores: Numerical analysis and application to the fluorescent protein dronpa," *J. Amer. Chem. Soc.*, vol. 129, no. 51, pp. 16 132–16 141, 2007.
[37] J. Yang, C. Dong, Y. Dong, S. Liu, L. Pan, and C. Zhang, "Logic nanoparticle beacon triggered by the binding-induced effect of multiple inputs," *ACS Appl. Mater. Interfaces*, vol. 6, no. 16, pp. 14 486–14 492, 2014.